Optimal Foot Trajectory Planning of Bipedal Robots Based on a Measure of Falling

Regular Paper

Byoung-Ho Kim[1,*]

1 Biomimetics & Intelligent Robotics Lab., Dept. of Mechatronics Engineering, Kyungsung University, Nam-gu, Busan, South Korea
* Corresponding author E-mail: kimbh@ks.ac.kr

Abstract This paper presents a falling-based optimal foot trajectory planning method (FOFTP) for the effective walking of bipedal robots in three-dimensional space. Our primary concern is to determine the optimal footstep location for the more balanced walking of bipedal robots based on a measure of falling. A proper strategy for the intermediate trajectory of the swing foot is also considered. The feasibility of the FOFTP method is verified by a typical bipedal walking simulation. We also discuss the walking efficiency of the proposed approach. It is finally shown that the proposed foot trajectory planning method is applicable for the effective walking of bipeds or humanoid robots.

Keywords Foot trajectory planning, Bipedal robots, Measure of falling

1. Introduction

It is well-known that the part of foot trajectory planning is crucial for the walking strategies of bipeds or humanoid robots.[1–8] Thus, this paper concerns on effective foot trajectory planning which enables bipedal robots to walk in a more natural fashion.

In fact, there exist many kinds of walking patterns according to the given mobile manipulation tasks at hand. In order to plan a walking pattern of for bipeds or humanoid robots, the conventional zero-moment point approach has been employed by many researchers.[9–11] This approach concerns on the trajectory of the body based on the reference trajectory assigned at the foot space. A predictive control approach for a walking gait's generation was proposed by Diedam et al.[12] Their contribution is was to employ an adaptive foot positioning scheme in despite of its rather large computational costs to improve the dynamic balance in a the walking process. In order to compute the optimal sequences of footstep positions, some footstep planning approaches were presented.[7,8] This approach is advantageous for footstep planning among obstacles. Also, there exist some gait generation approaches based on energy saving[13] and gradient methods.[14] On the other hand, Yun et al.[15] recently presented a falling strategy for

the safety of humanoid robots, where they addressed on a falling direction change for effective falling through a stepping approach. Since safety is the primary issue for humanoid robots to freely exist in human space and a fall from a walking posture can cause damage to the robot as well as to delicate and expensive objects in the surroundings or human beings, it is quite remarkable to consider the deliberate falling problem for a safe fall.[16] In this sense, a predictive control considering viability can be a useful approach for safe and effective locomotion.[17] Also, some types of measures have been proposed for balance in bipedal walking.[18,19] However, comprehensive studies of bipedal walking pattern generation considering falling remain rare. Thus, we pay attention to a simple measure of falling to identify a more effective walking configuration for bipeds or humanoid robots.

The objective of this paper is to present a falling-based optimal foot trajectory planning method for the effective walking of bipeds or humanoid robots, where a new measure of falling is employed for this purpose. This paper is organized as follows. In Section 2, we specify a virtual-legged walking model of bipedal robots. A falling-based optimal foot trajectory planning method is described in Section 3. In Section 4, simulation results for bipedal walking are shown to illustrate the feasibility of the proposed foot trajectory planning method. Finally, concluding remarks are drawn in Section 5.

2. Modelling of Bipedal Walking Robots

In the field of bipeds or humanoid robots, shown in Figure 1, foot trajectory planning is fundamentally important for effective walking and manipulation tasks. To deal with such an effective bipedal walking problem, we consider a bipedal robot simplified as in Figure 2(a) and we also make a virtual-legged (VL1 and VL2) walking model for the bipedal robot, as shown in Figure 2(b).

In this paper, the virtual-legged bipedal model is used to identify the outstanding characteristics of bipedal robots in terms of balanced walking. Such a form of bipedal walking is usually performed by using one of the two legs alternatively. If a leg moves, the other leg should support the robot system to achieve the desired walking gait. The position of each foothold might have a serious effect on the balance of the robot system in the walking process. As such, in order to confirm such bipedal motion factors, we describe the force relationships of the bipedal walking mechanism, shown in Figure 2(b), as follows:

$$m\ddot{x}_c = f_x \tag{1}$$

$$m\ddot{y}_c = f_y \tag{2}$$

$$m\ddot{z}_c = f_z - mg \tag{3}$$

where m, $\ddot{x}_c$, $\ddot{y}_c$ and $\ddot{z}_c$ represent the total point mass, the x-, y- and z-directional accelerations at the centre of mass (COM) of the robot system, respectively. The parameters f_x and f_y denote the force components for the robot in going towards the x- and y-directions and f_z implies the vertical supporting force for the robot. The parameter $g(=9.8\text{m/s}^2)$ represents the gravitational acceleration coefficient.
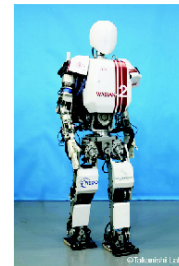

Figure 1. A humanoid robot, WABIAN-2R[3]

Also, the x-, y- and z-directional moments observed at the centre of the sole, τ_x, τ_y and τ_z, can be represented by:

$$\tau_x = -z_c m\ddot{y}_c + (y_c - y_{fi})m\ddot{z}_c + (y_c - y_{fi})mg \tag{4}$$

$$\tau_y = z_c m\ddot{x}_c - (x_c - x_{fi})m\ddot{z}_c - (x_c - x_{fi})mg \tag{5}$$

$$\tau_z = -(y_c - y_{fi})m\ddot{x}_c + (x_c - x_{fi})m\ddot{y}_c \tag{6}$$

where these moments are to be activated by the reaction force and the gravitational force. The parameters x_c, y_c and z_c represent the moving trajectory of the COM of the body of the robot in the x-, y-, and z-directions, respectively. The corresponding directional position of the i-th supporting foot is denoted by x_{fi}, y_{fi} and z_{fi}. In practice, those components enable us to know the importance of the current foot position for effective bipedal walking.

By rearranging the force and moment relations given by (1)~(6), we have a vector-matrix form of the dynamic equation, as follows:

$$f = A\ddot{p}_c + Bp_c + Cp_{fi} + dg \tag{7}$$

where the generalized force vector $f \in R^{6 \times 1}$, the position vector of the COM $p_c \in R^{3 \times 1}$ and its acceleration vector $\ddot{p}_c \in R^{3 \times 1}$, the position vector of the i-th supporting foot $p_{fi} \in R^{3 \times 1}$, and the gravitational effect vector $d \in R^{6 \times 1}$, respectively, can be expressed by:

$$f = \begin{bmatrix} f_x & f_y & f_z & \tau_x & \tau_y & \tau_z \end{bmatrix} \tag{8}$$

$$p_c = \begin{bmatrix} x_c & y_c & z_c \end{bmatrix} \tag{9}$$

$$\ddot{p}_c = \begin{bmatrix} \ddot{x}_c & \ddot{y}_c & \ddot{z}_c \end{bmatrix} \tag{10}$$

$$p_{fi} = \begin{bmatrix} x_{fi} & y_{fi} & z_{fi} \end{bmatrix} \tag{11}$$

$$d = \begin{bmatrix} 0 & 0 & m & 0 & 0 & 0 \end{bmatrix}. \tag{12}$$

Moreover, the dynamic mapping matrix $A \in R^{6 \times 3}$, the mapping matrix between the position of the COM and the generalized force $B \in R^{6 \times 3}$ and the mapping matrix between the position of the supporting foot and the generalized force $C \in R^{6 \times 3}$ can be represented by:
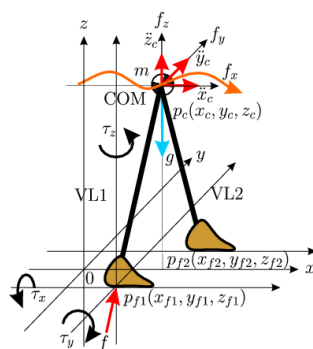
$$A = \begin{bmatrix} m & 0 & 0 \\ 0 & m & 0 \\ 0 & 0 & m \\ 0 & -z_c m & (y_c - y_{fi})m \\ z_c m & 0 & -(x_c - x_{fi})m \\ -(y_c - y_{fi})m & (x_c - x_{fi})m & 0 \end{bmatrix} \tag{13}$$

$$B = \begin{bmatrix} 0 & 0 & 0 & 0 & -mg & 0 \\ 0 & 0 & 0 & mg & 0 & 0 \\ 0 & 0 & 0 & 0 & 0 & 0 \end{bmatrix}^T \tag{14}$$

$$C = \begin{bmatrix} 0 & 0 & 0 & 0 & mg & 0 \\ 0 & 0 & 0 & -mg & 0 & 0 \\ 0 & 0 & 0 & 0 & 0 & 0 \end{bmatrix}^T. \tag{15}$$
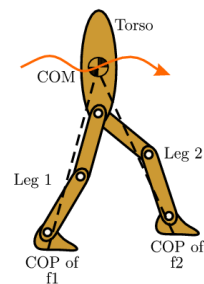
(a) A bipedal robot

(b) A virtual-legged bipedal walking model

Figure 2. An effective model of bipedal walking robots

From (7)~(15), it is noted that the roll motion of the bipedal robot is affected by the y- and z-directional accelerations of the centre of mass and that the pitch motion is dependent on the x- and z-directional accelerations. They are also dependent on the relative locations of the supporting foot and the centre of mass. The yaw motion is especially dependent on the relative locations of the supporting foot and the centre of mass as well as the x- and y-directional accelerations. Since the relative distance between the supporting foot and the centre of mass is indispensable for the robot in walking, the yaw motion is a natural action when bipeds walk. Such a fluctuating yaw motion is experienced easily in the walking behaviour of humans. In the case of a walk with long strides, especially, those momental actions will be modulated significantly. In particular, excessive momental actions may give rise to the imbalance of the bipedal biped in walking.

As a result, it is noted that a strategy for effective footstep positioning can contribute ultimately to balance in bipedal walking.

3. Foot Trajectory Planning

This section describes a new foot trajectory planning method based on a falling-based optimization technique. Our approach has two methodologies to plan the swing foot's trajectory, as follows. One is a footstep planner, where an optimization technique using a measure of falling is used to determine the upcoming footstep location of the swing leg. The other is a trajectory planner to determine the intermediate location between the starting position of the swing foot and the upcoming footstep position assigned by the footstep planner.

3.1 State of Falling

For a new foot trajectory planning method, we first define a falling concept for bipedal robots. Consider a walk volume V_c, shown in Figure 3, which implies the reachable region of the virtual leg mechanism on a walk. In practice, the virtual leg is reachable within the range of $r_{\min} \leq r \leq r_{\max}$ due to the limitation of the real joint actuation of the bipedal robot. In this paper, the state of falling is defined as that state where the virtual leg has fallen down on the ground surface in the xy plane of Figure 3.
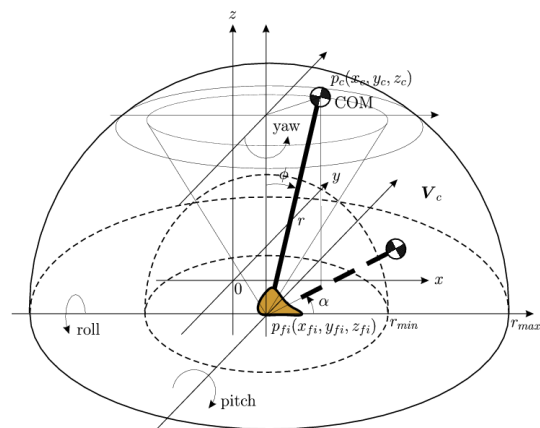

Figure 3. Walk volume of the virtual leg mechanism

ϕ (degree)	State of falling	Remarks
0	No fall	Standing upright
$0<\phi<90$	Marginal state as ϕ	On walking
90	Fall down	Out of walking

Table 1. Classification of the state of falling

Based on the definition of falling, the angle parameter ϕ in Figure 3 is directly related to the degree of falling of the robot. Accordingly, the angle is considerable as a simple identifier for the current state of falling of the robot. Table 1 shows the state of falling in the planar space. In addition, the direction of falling can be known by the yaw angle parameter α.

3.2 Optimal Foot Trajectory Planning Method

The foot trajectory planning problem considered in this paper can be depicted as Figure 4 and its actual goal is to determine the optimal footstep location providing support for the robot to walk along the trajectory prescribed in the COM space. This approach is meaningful for the task-based mobile manipulation of bipeds or humanoid robots, and it is different from the conventional ZMP-based methods.[10,11] In order to plan the swing foot's trajectory, we propose a new footstep planner using an optimization technique based on a measure of falling.

In addition, we use a trajectory planner to determine the intermediate location between the starting position of the swing foot and the upcoming footstep position assigned by the footstep planner.
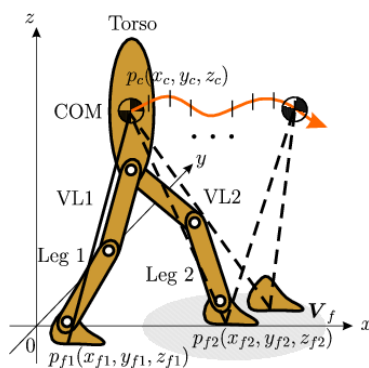

Figure 4. Foot trajectory planning of a bipedal robot

In fact, many kinds of approaches can be used for the second purpose. In this paper, we utilize the conventional cubic trajectory planning method which is useful for a single smooth motion.[20] By using the cubic trajectory planning method, it is possible to generate a certain directional trajectory u as follows:

$$u = a_0 + a_1 t + a_2 t^2 + a_3 t^3 \qquad (16)$$

where t represents the time variable and the coefficients $a_i (i=0,\cdots,3)$ are given by $a_0 = s_i$, $a_1 = 0$, $a_2 = 3(s_f - a_0)/t_f^2$ and $a_3 = -2(s_f - a_0)/t_f^3$, where t_f represents the ending time of the trajectory. The parameters s_i and s_f denote the starting and goal positions of the trajectory. For convenience, the cubic trajectory function given by (16) can be rewritten by:

$$u = \mathbf{traj}\left(s_i,\ s_f,\ t,\ t_f\right). \qquad (17)$$

When the bipedal robot in Figure 4 lifts the left leg (VL2) to walk, the robot system is managed mainly by the right leg (VL1) for the desired walking motion. In such a walking situation, one of requirements for the robot is how to assign the next footstep location of the swing leg. For this, we propose an optimization technique using a new measure of falling.

The measure of falling proposed in this paper is as follows. It is defined as the total of the falling index for the foothold candidates selected at each stage of walking. In particular, the measure of falling $I_{fall,k}$ for the k-th footstep within the available search space V_f is computed by:

$$I_{fall,k} = \sum_{j=1}^{n_c} \frac{\phi_{jk}}{\phi_{\max}}, k = 1,\cdots,n_f \qquad (18)$$

where n_c denotes the number of trajectory samples prescribed at the COM space and n_f represents the number of the next footstep candidates for the swing leg. The parameter $\phi_{\max}$ is the maximum falling angle for a normalization and it can be set as 90° in the planar walking surface, as shown in Figure 3. The angle of falling ϕ_{jk} is calculated by:

$$\phi_{jk} = \tan^{-1}\left(\frac{\sqrt{r_{x,jk}^2 + r_{y,jk}^2}}{r_{z,jk}}\right) \qquad (19)$$

where $r_{x,jk}$, $r_{y,jk}$ and $r_{z,jk}$ imply the x-, y- and z-directional distances between the j-th position of the COM trajectory and the origin of the k-th foothold candidate of the swing leg, respectively.

As a result, the proposed optimal foot trajectory planning strategy can be summarized as follows: find the upcoming footstep positions of the swing foot in the x-, y- and z-directions that minimize the measure of falling given by (18) for all the footstep candidates to support the COM trajectory, predefined at each stage of walking according to the given mobile manipulation task. If the goal position of the swing foot is accordingly determined at each starting moment of walking, the intermediate foot

trajectory between the current foothold and the next foothold is generated by using the cubic trajectory planning method given by (17).

4. Simulation and Discussion

This section performs a simulation of a *typical* bipedal walking task using the falling-based optimal foot trajectory planning method described in Section 3 and it offers significant results to verify the feasibility of the proposed method.

4.1 Bipedal Walking Task and Foot Trajectory Planning

There exists a preferable walking style for bipedal robots to achieve a specific mobile manipulation task. It is highly dependent on the desired behaviour of the body. For an illustrative simulation, we predetermined a *typical* motion trajectory in the COM space for bipedal manipulation, as shown in Figure 4, and then tried to plan the foot trajectory providing for the desired COM trajectory. In order to assign the desired COM trajectory, we considered a human-like sequential walking style mimicking the normal behaviour of human walking.[21] It is summarized as follows:

1. START.
2. Homing action for the initial upright posture standing in a state of dual support (DS).
3. Shift the body to the right for the shifting time t_{shift} while maintaining DS.
4. Lift the left foot and move it to the next foot position for $T - t_{shift}$ by keeping the right foot support (RS), where T is the time period for one step motion.
5. Shift the body to the left for t_{shift} while maintaining DS.
6. Lift the right foot and move it to the next foot position as with the third phase.
7. If the walking task is finished, STOP after homing. Otherwise, return to the step 3.

Figure 5 shows the motion trajectories prescribed in the COM space for a bipedal walking simulation considering the human-like walking style. Specifically, in order for the robot to take a step forward, the *x*-directional trajectory of the COM x_c was assigned as Figure 5(a). It was made by using the cubic trajectory planning method given by (17), where the size of movement at each step is updated by as much as 0.08m. Figure 5(b) shows the *y*-directional trajectory of the COM which has been planned by employing (17) properly as the corresponding section. The words RS, LS, and DS imply the state of the robot system supported by the right, left, or both feet, respectively. The time period for one step motion was set arbitrarily as 1s. The parameter t_{shift} represents a time

zone for the body to shift while maintaining the posture of dual support. It is actually helpful for an effective walk, where it was set as 0.4s. In fact, the robot takes a step forward after the shifting time. The *z*-directional trajectory z_c was also assigned by employing (17), as shown in Figure 5(c). Of course, the trajectories specified in this paper can be formed differently according to the bipedal manipulation task as given.
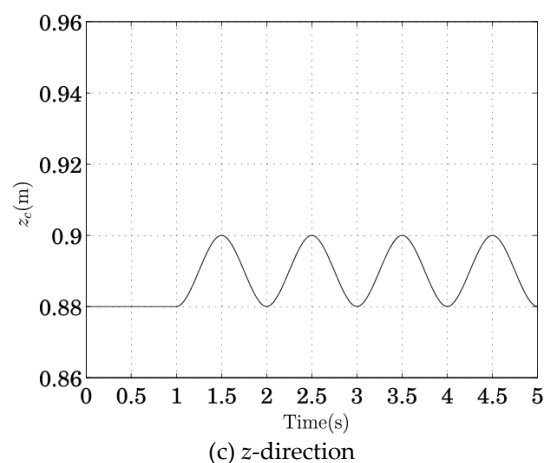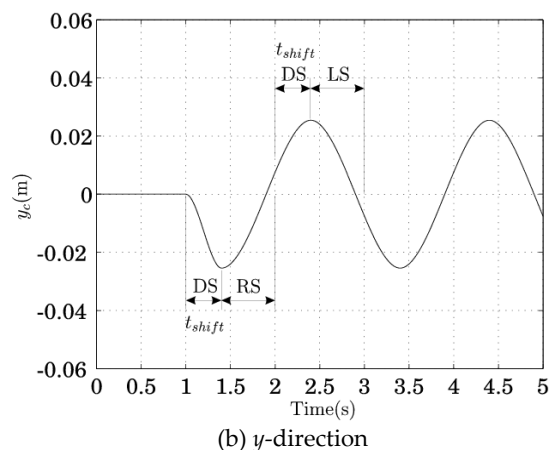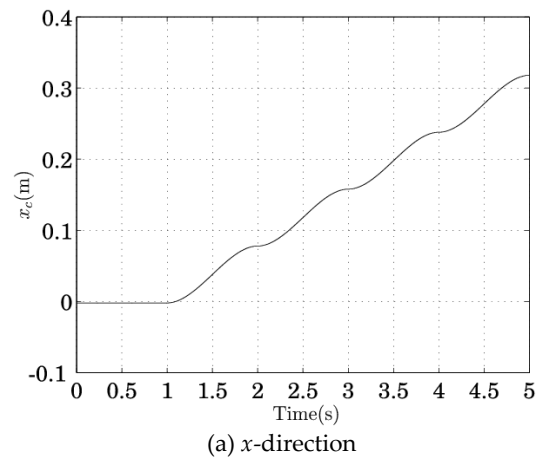

(a) *x*-direction

(b) *y*-direction

(c) *z*-direction

Figure 5. Motion trajectories prescribed in the COM space for bipedal manipulation, where the assigned homing action to adjust the initial posture of the robot is performed until 1s.
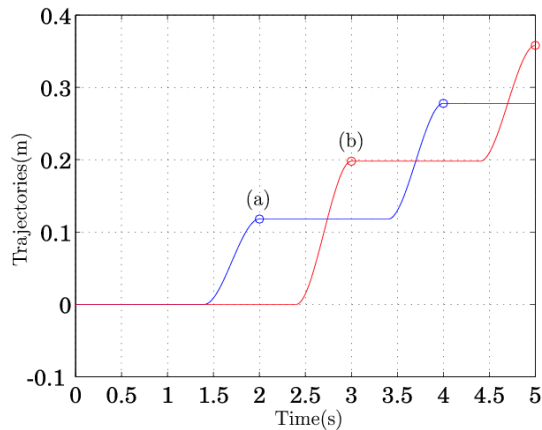
Figure 6. Trajectories of the two feet planned for the *x*-directional motion: (a) left foot and (b) right foot.

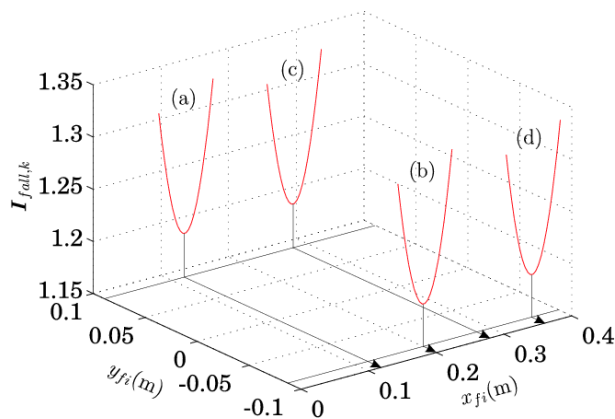**Figure 7.** Identifying the corresponding optimal footstep location at each stage of walking based on the measure of falling: (a) x_{f2} =0.12m (left foot), (b) x_{f1} =0.2m (right foot), (c) x_{f2} =0.28m, and (d) x_{f1} =0.36m.

Next, we describe the results of foot trajectory planning for the walking task given by Figure 5.

Figure 6 shows the resultant trajectories of the two feet planned for *x*-directional motion, where the circle 'o' indicates the upcoming footstep location of each foot planned by the optimization technique using the measure of falling given by (18). For the purpose of the optimization, the size of each walking step has been assigned as the same size of movement of the body at each step. We considered twenty footstep candidates at each step and twenty trajectory samples of one step motion at the COM space. That is to say, the parameters of n_c and n_f in (18) have been assigned for the optimization as an arbitrary value of 20. By using those parameters, each walking and motion step has been divided by the same distance. Figure 7 shows the profiles of the measure of falling checked in the process of walking. They have been used to determine the corresponding *x*-directional footstep location for the periodic bipedal walking and, from Figure 7, it is possible to identify the optimal footstep location for continuous

walking. Physically, the selected footholds are optimal in terms of the overall balance at each stage of walking. The intermediate trajectory of the swing foot has been determined by (16). From Figure 5(b) and Figure 6, it is confirmed that there exist three modes of walking, namely RS, DS and LS.

Since the assigned task is a kind of straightforward bipedal walk, the *y*-directional trajectories of the two feet have been planned as y_{f1} =-0.089m and y_{f2} =0.089m, which are initialized for the right foot and the left foot, respectively. The *z*-directional trajectory of the swing foot has been planned as Figure 8. It was made by a kind of half-sine function activated at each step of walking.
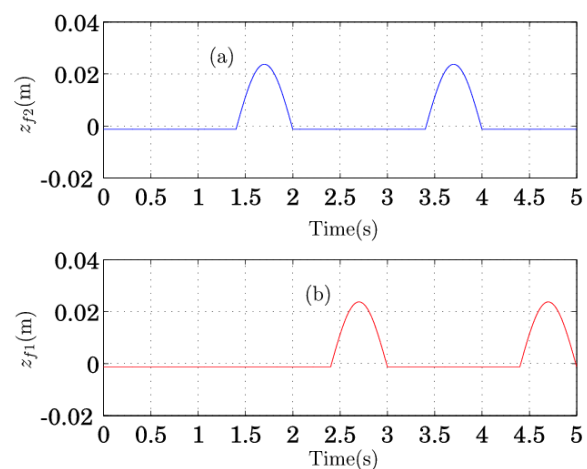

Figure 8. Trajectories of the two feet planned for the *z*-directional motion: (a) left foot and (b) right foot.

4.2 Results of Walking Simulation

To illustrate the feasibility of the falling-based optimal foot trajectory planning method, we performed the three-dimensional walking task assigned in the previous section. For this simulation, we employed the bipedal robot system shown in Figure 9.
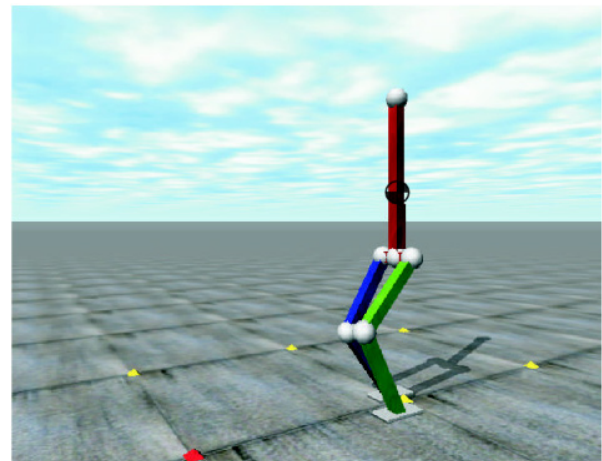

Figure 9. A bipedal walking robot used in the simulation

Item	Specification	Units
Position of COM	0.95	m
Length of torso	0.80	m
Length of each thigh	0.39	m
Length of calf	0.38	m
Weight of torso	50.00	kg
Weight of each thigh	5.68	kg
Weight of each calf	6.90	kg

Table 2. Physical parameters of the bipedal robot

The robot system consists of five rigid links, such as a torso, two thighs, and two calves. It has twelve degrees of freedom: two for each hip, one for each knee, and three for each ankle. There exists a roll and a pitch joint at each hip, a pitch joint at each knee, and three joints for the roll, pitch and yaw motions at each ankle. Table 2 shows the physical parameters of the robot system. The position of the centre of mass indicates the distance measured from the ground when the robot is standing straight at in the initial state.
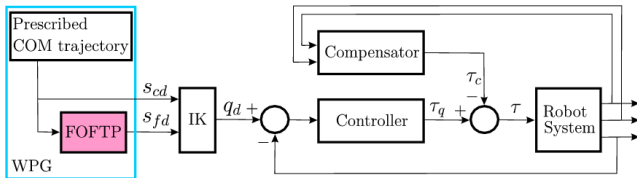

Figure 10. Control block diagram for the bipedal walking task

The control block diagram for the bipedal walking task is shown in Figure 10. The walking pattern generator (WPG) in Figure 10 has two roles. One is to prescribe the trajectory(s_{cd}) in the COM space shown in Figure 5 and the other is to generate the trajectory of each foot s_{fd} required for the robot in following the trajectory prescribed in the COM space. For the walking control of the robot, we employed a typical proportional and derivative joint controller with the gain matrices of $K_p\left(\in R^{12\times12}\right)=\mathbf{diag}\left(300,\ \cdots,\ 300\right)$ and $K_d\left(\in R^{12\times12}\right)=\mathbf{diag}\left(30,\ \cdots,\ 30\right)$ for all the joints, respectively. The desired joint angles for the joint controller have been made by the process of general inverse kinematics (IK). Also, we used a compensator to consider the dynamic effects at the hip space as follows:

$$\tau_c = D_h I_h \left(200\varphi + 0.5\omega\right) \tag{20}$$

where $D_h\left(\in R^{12\times3}\right)$ denotes the dynamic translation matrix relating the hip space to the joint space, and $\varphi\left(\in R^{3\times1}\right)$ and $\omega\left(\in R^{3\times1}\right)$ represent the Euler angle and the angular velocity vectors of the torso, respectively. The total inertial tensor represented in the hip space $I_h\left(\in R^{3\times3}\right)$ has been set by $\mathbf{diag}\left(22.227, 19.976, 3.092\right)$. The reaction forces for the two feet have been calculated by typical stiffness modelling.

Figure 11(i) shows the trajectory tracking result for the three-dimensional walking motion in the COM space of the bipedal robot. The performances in roll and pitch directions have been plotted in Figures 11(ii) and (iii).
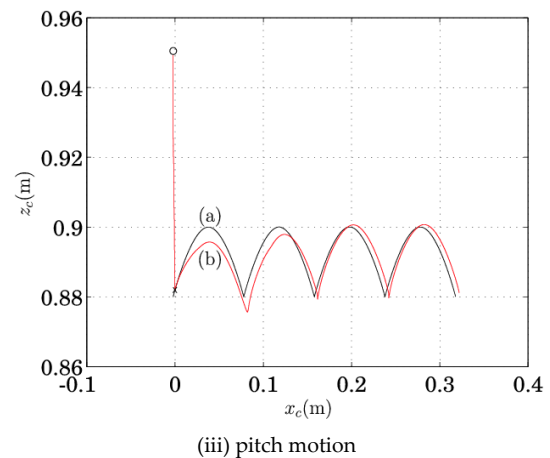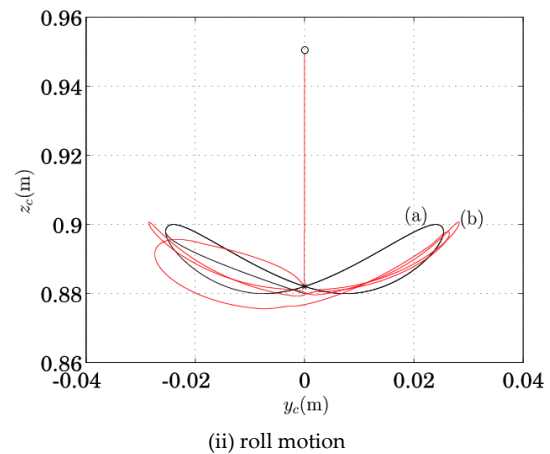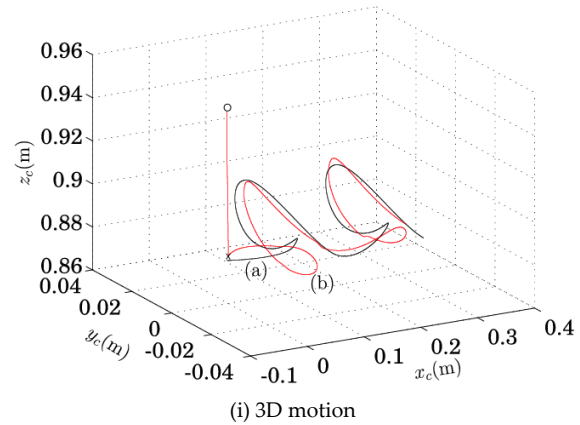

(i) 3D motion

(ii) roll motion

(iii) pitch motion

Figure 11. Trajectory following result for the three-dimensional walking motion in the COM space, where the section between 'o' and 'x' implies the homing action for the initial configuration of the bipedal robot: (a) desired trajectory and (b) actual trajectory.
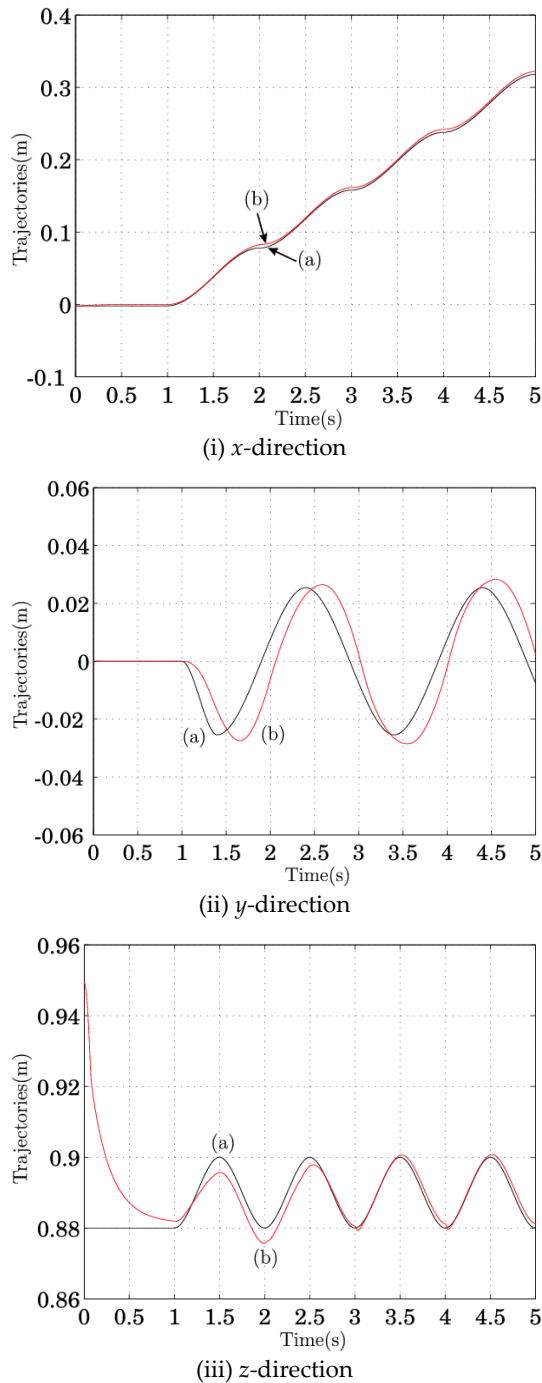
Figure 12. Trajectory following results in the COM space: (a) desired trajectory and (b) actual trajectory.

To be more specific, we can confirm the reasonable *x*-, *y*- and *z*-directional motions in the COM space by Figure 12. The stage up until *t*=1s in Figure 12 represents the homing action assigned for the robot in taking its initial posture. In particular, the *z*-directional motion is an important pattern for bipedal robots in exhibiting more natural walking behaviour. In the conventional study on the walking pattern generation of a bipedal robot,[11] however, the body motion was confined to the two-dimensional space only and, thus, such a vertical motion - as shown in Figure 12(iii) - occurring in the normal walking of bipeds or humanoid

robots cannot be observed. Recently, the issue of stable bipedal walking has been addressed.[22] However, the motion in the sagittal plane was limited by using a radial bar. In this case, the rolling motion created by the *y*-directional shaking cannot be considered and the complete stability of the bipedal walking may not be analysed. This is because the physical moments generated by the walking style can have a serious impact on the walking balance of the bipedal robot system.[23]
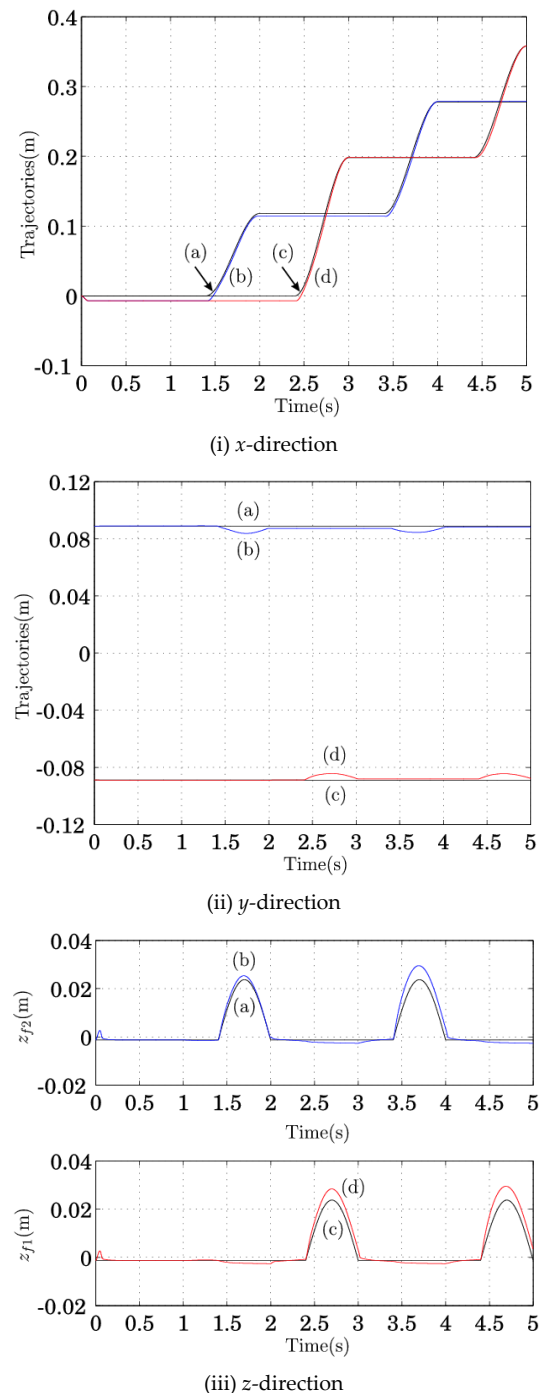

Figure 13. Trajectory following results of the two feet: (a) desired trajectory of the left foot, (b) actual trajectory of the left foot, (c) desired trajectory of the right foot, and (d) actual trajectory of the right foot.

From Figure 13, we can also confirm the successful x-, y- and z-directional walking trajectory results of each foot for the given task. Figure 14 shows the satisfactory trajectories of the knee joints of the robot for the given walking task. We can also confirm that the step motions of walking are reasonable by observing the pattern of the vertical reaction force of each foot, as shown in Figure 15.
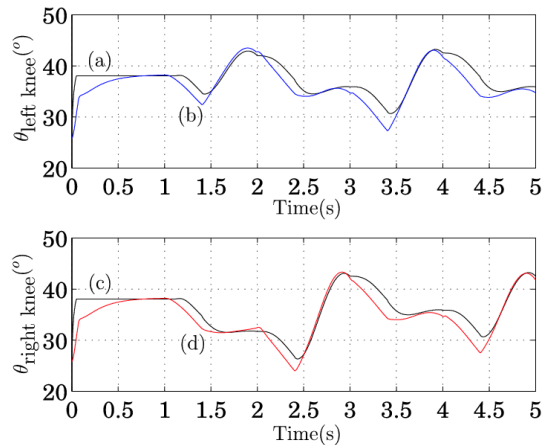

Figure 14. Trajectory following results of the knee joints: (a) desired trajectory of the left knee, (b) actual trajectory of the left knee, (c) desired trajectory of the right knee, and (d) actual trajectory of the right knee.
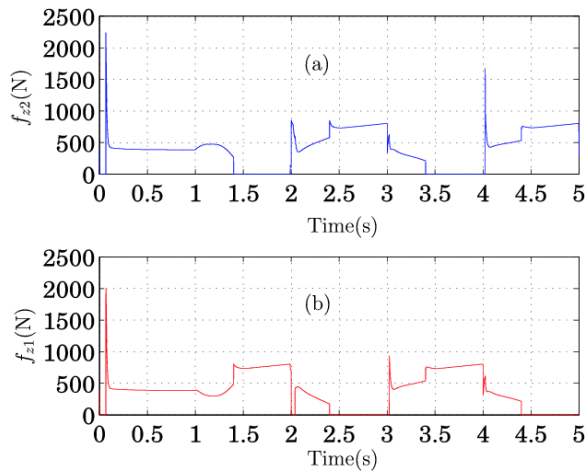

Figure 15. Reaction force of each foot on the z-axis: (a) left foot and (b) right foot.

Case	Time(s)	x_{f2} (m)	x_{f1} (m)	Remarks
1	1.0	0.12	0.00	Planned by the proposed method
	2.0	0.12	0.20	
	3.0	0.28	0.20	
	4.0	0.28	0.36	
2	1.0	0.18	0.00	Assigned arbitrarily
	2.0	0.18	0.26	
	3.0	0.34	0.26	
	4.0	0.34	0.40	

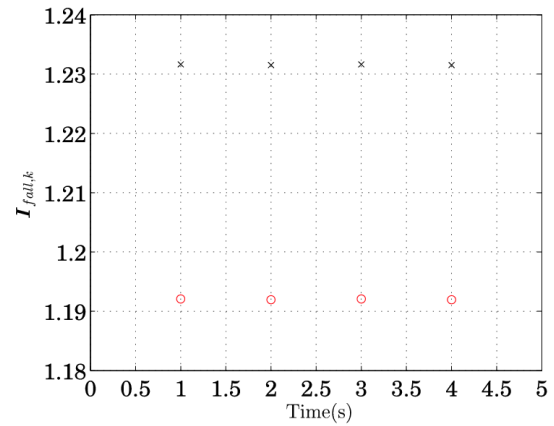**Table 3.** The landing locations of the two feet for the walking task

Figure 16. Comparison of the measure of falling, where 'o' indicates case 1 (proposed case) and 'x' is case 2.
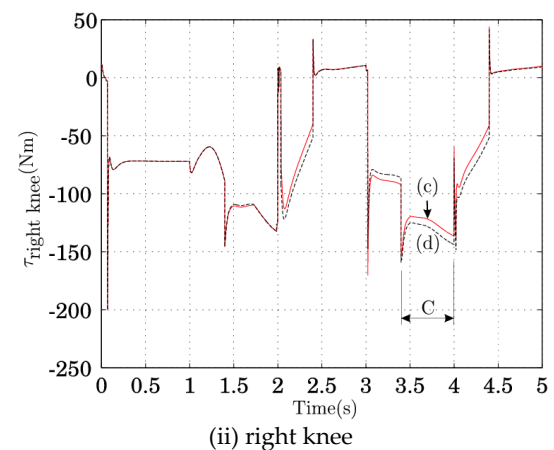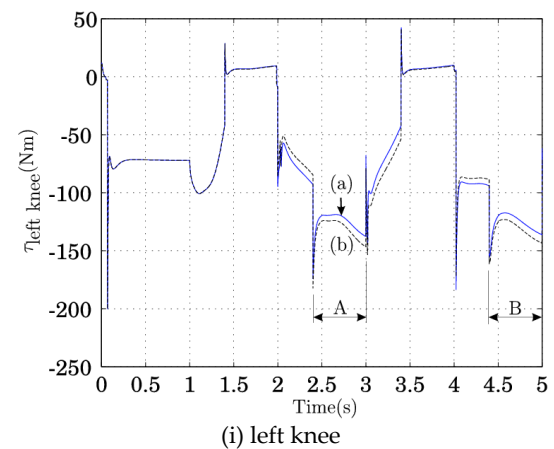

(i) left knee

(ii) right knee

Figure 17. Torque profiles of the knee joints: (a) torque of the left knee for case 1 (proposed case), (b) torque of the left knee for case 2, (c) torque of the right knee for case 1, and (d) torque of the right knee for case 2.

Next, and in order to show the walking efficiency of the proposed approach, we performed an additional simulation by only changing just the landing positions of the swing foot, as in Table 3. The first case is based on the proposed optimal foot trajectory planning method and the second case is seeks to assign the landing position of the swing foot in near the optimal position arbitrarily.

Byoung-Ho Kim: Optimal Foot Trajectory Planning of Bipedal Robots Based on a Measure of Falling

Figure 16 shows the measures of falling- given by (18) - evaluated by this simulation, where the measure by of the proposed optimal case is more or less than that of the case 2. This means that the overall balance of the walking configuration planned by the proposed method is basically better.

Since the knee joints play an important role to in supporting the bipedal walking motion, identifying the torque profiles of the knee joints is also valuable to in analyze analysing the walking efficiency of the proposed approach. In this sense, we especially notably showed the torque profiles of the knee joints for the given walking task, as shown in Figure 17. The sections of A, B, and C in Figure 17 indicate the ranges that the swing foot is maintained after touch down on the ground and the corresponding leg mechanism should support the motion of the walking system. As a result, we can confirm that the torque of the knee joint in the case 1 is more or less than that of the case 2, particularly especially in those supporting situations indicated by A, B, and C. This implies that the walking planned by the proposed approach is more efficient in terms of the energy required in by the knee.

Through the simulation, it is confirmed that the simulation robot walked stably from the responses in Figure 11, and from Figures 12 and 13 the resultant tracking performances of the walking task are satisfactory. According to (7)~(13), it is actually possible to moderate the momental actions of the bipedal robot system by optimizing the location of footholds. Thus, it is noted that successful results could be obtained by taking the optimal footholds for bipedal walking. In addition, the *y*-directional foot step planning is also important for the side walking of bipedal robots. It can be achieved by the same procedure as described in this paper.

5. Concluding Remarks

This paper presented an optimal foot trajectory planning method for the effective walking of bipedal robots, where a new measure of falling has been used to estimate optimal footholds. The feasibility of the proposed foot trajectory planning method has been verified by simulations for a *typical* bipedal walking task. The simulation results showed the successful tracking performances of the bipedal robot for the given walking task and the walking efficiency of the proposed approach has been confirmed. It is also confirmed through the simulation whereby the falling-based foothold searching technique is useful for identifying a more effective walk configuration in terms of balance. Consequently, it is expected that the proposed foot trajectory planning method can be applied to bipedal robots for effective walking and manipulation.

In addition, a proper consideration of an irregular walking surface will be an important matter for more natural bipedal walking and the running pattern of bipedal robots will be interesting for further study.

6. Acknowledgements

7. References

[1] K. Hirai, M. Hirose, Y. Haikawa, and T. Takenaka, "The development of Honda humanoid robot," Proc. of IEEE Int. Conf. on Robotics and Automation, pp. 1321-1326, 1998.

[2] Y. Sakagami, R. Watanabe, C. Aoyama, S. Matsunaga, N. Higaki, and K. Fujimura, "The intelligent ASIMO: system overview and integration," Proc. of IEEE/RSJ Int. Conf. on Intelligent Robots and Systems, pp. 2478-2483, 2002.

[3] Y. Ogura, H. Aikawa, K. Shimomura, H. Kondo, A. Morishima, H.-O. Lim, and A. Takanishi, "Development of a new humanoid robot, WABIAN-2," Proc. of IEEE Int. Conf. on Robotics and Automation, pp. 2478-2483, 2002.

[4] K. Kanako, F. Kanehiro, S. Kajita, K. Yokoyama, K. Akachi, T. Kawasaki, S. Ota, and T. Isozumi, "Design of prototype humanoid robotics platform for HRP," Proc. of IEEE/RSJ Int. Conf. on Intelligent Robots and Systems, pp. 2431-2436, 2002.

[5] I. W. Park, J.-Y. Kim, J. Lee, and J.-H. Oh, "Mechanical design of humanoid robot platform KHR-3 (KAIST humanoid robot-3: HUBO)," Proc. of IEEE-RAS Int. Conf. on Humanoid Robots, pp. 321-325, 2005.

[6] Mizuuchi, T. Yoshikai, Y. Sodeyama, Y. Nakanishi, A. Miyadera, T. Yamamoto, T. Niemela, M. Hayashi, J. Urata, Y. Namiki, T. Nishino, and M. Inaba, "Development of musculoskeletal humanoid Kotaro," Proc. of IEEE Int. Conf. on Robotics and Automation, pp. 82-87, 2006.

[7] J. Kuffner, K. Nishiwaki, S. Kagami, M. Inaba, and H. Inoue, "Footstep planning among obstacle for biped robots," Proc. of IEEE/RSJ Int. Conf. on Intelligent Robots and Systems, pp. 500-505, 2001.

[8] J. Chestnutt, M. Law, G. Cheung, J. Kuffner, J. Hodgins, and T. Kanade, "Footstep planning for the Honda ASIMO humanoid," Proc. of IEEE Int. Conf. on Robotics and Automation}, pp. 631-636, 2005.

[9] M. Vukobratovic and J. Stepaneko, "On the stability of anthropomorphic systems," Mathematical Biosciences, Vol. 15, pp. 1-37, 1972.

[10] T. Sugihara, Y. Nakamura, and H. Inoue, "Realtime humanoid motion generation through ZMP manipulation based on inverted pendulum control," Proc. of IEEE Int. Conf. on Robotics and Automation, pp. 1404-1406, 2002.

[11] S. Kajita, F. Kanehiro, K. Kaneko, K. Fujiwara, K. Harada, K. Yokoi, and H. Hirukawa, "Biped walking pattern generation by using preview control of zero-moment point," Proc. of IEEE Int. Conf. on Robotics and Automation, pp. 1620-1626, 2003.

[12] H. Diedam, D. Dimitrov, P.-B. Wieber, K. Mombaur, and M. Diehl, "Online walking gait generation with adaptive foot positioning through linear model predictive control," Proc. of IEEE/RSJ Int. Conf. on Intelligent Robots and Systems, pp. 1121-1126, 2008.

[13] M. Uemura, K. Kimura, and S. Kawamura, "Generation of energy saving motion for biped walking robot through resonance-based control method," Proc. of IEEE/RSJ Int. Conf. on Intelligent Robots and Systems, pp. 2928-2933, 2009.

[14] K. Nagasaka, M. Inaba, and H. Inoue, "Walking pattern generation for a humanoid robot based on optimal gradient method," Proc. of IEEE Int. Conf. on Systems, Man, and Cybernetics, 1999.

[15] S.-K Yun, A. Goswami, and Y. Sakagami, "Safe fall: humanoid robot fall direction change through intelligent stepping and inertia shaping," Proc. of IEEE Int. Conf. on Robotics and Automation, pp. 781-787, 2009.

[16] K. Ogata, K. Terada, and Y. Kuniyoshi, "Real-time selection and generation of fall damage reduction actions for humanoid robots," Proc. of IEEE-RAS Int. Conf. on Humanoid Robots, pp. 233-238, 2008.

[17] P.-B. Wieber, "Viability and predictive control for safe locomotion," Proc. of IEEE/RSJ Int. Conf. on Intelligent Robots and Systems, pp. 1103-1108, 2008.

[18] D. G. E. Hobbelen and M. Wisse, "A disturbance rejection measure for limit cycle walkers: the gait sensitivity norm," IEEE Trans. on Robotics, Vol. 23, No, 6, pp. 1213-1224, 2007.

[19] D. L. Wight, E. G. Kubica, and D. W. L. Wang, "Introduction of the foot placement estimator: a dynamic measure of balance for bipedal robotics," Jour. of Computational and Nonlinear Dynamics, Vol. 3, Issue 1, January 2008.

[20] J. J. Craig, Introduction to robotics mechanics and control, 3rd. edt., Prentice Hall, 2004.

[21] A. D. Kuo, "Choosing your steps carefully," IEEE Robotics & Automation Magazine, pp. 18-29, June 2007.

[22] F. Plestan, J. W. Grizzle, E. R. Westervelt, and G. Abba, "Stable walking of a 7-DOF biped robot," IEEE Trans. on Robotics and Automation, Vol. 19, No. 4, pp. 653-668, 2003.

[23] B.-H. Kim, "Modeling and RPY motion analysis of bipedal walking robots," Jour. of Korean Institute of Intelligent Systems, Vol. 21, No. 3, pp. 353-358, 2011.